Supporting Information:

Controlling Surface Porosity of Graphene-based Printed Aerogels

Binghan Zhou[1], Zhuo Chen[1], Qian Cheng[2], Mingfei Xiao[1], Garam Bae[1], Dongfang Liang[2] and Tawfique Hasan[1]*

[1]*Cambridge Graphene Centre, University of Cambridge, Cambridge, CB3 0FA, UK*

[2]*Department of Engineering, University of Cambridge, Cambridge, CB3 0FA, UK*

Supplementary Table 1. A non-exhaustive survey of reported 3D printed graphene aerogel and their surface porosity.

Ink Precursor	Printing Methods	Surface Morphology	Reference
GO + AA	3D extrusion	Porous	*Adv. Mater.* 2018[1]
GO + Ca^{2+}	3D extrusion	Porous	*Adv. Funct. Mater.* 2018[2]
GO + SA	3D extrusion	Porous	*Adv. Funct. Mater.* 2018[3]
GO + Urea	3D extrusion	Porous	*ACS Nano* 2018[4]
GO + Silica + RF resin	Isooctane assisted printing	Non-porous	*Nat. Commun.* 2015[5]
GO + Silica + RF resin	Isooctane assisted printing	Non-porous	*Nano Lett.* 2016[6]
GO	Freeze-casting inkjet printing	Non-porous	*Small* 2016[7]
GO + Polymers	3D extrusion	Non-porous	*Adv. Mater.* 2018[8]
GO	3D extrusion	Non-porous	*J. Colloid Interface* Sci. 2019[9]
GO + HPMC	3D extrusion	Non-porous	*Adv. Mater.* 2020[10]

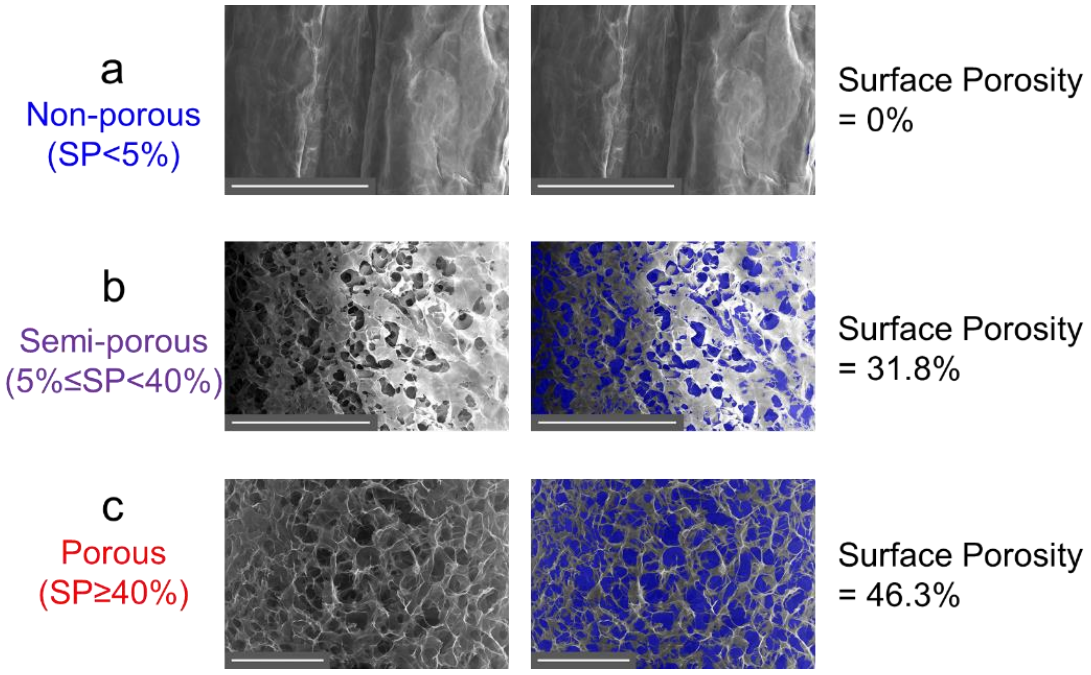

Supplementary Figure 1. Typical (a) non-porous, (b) semi-porous, and (c) porous graphene-based aerogel surfaces and corresponding surface porosity. Blue mask shows the porous area. Scale bars 100 μm.

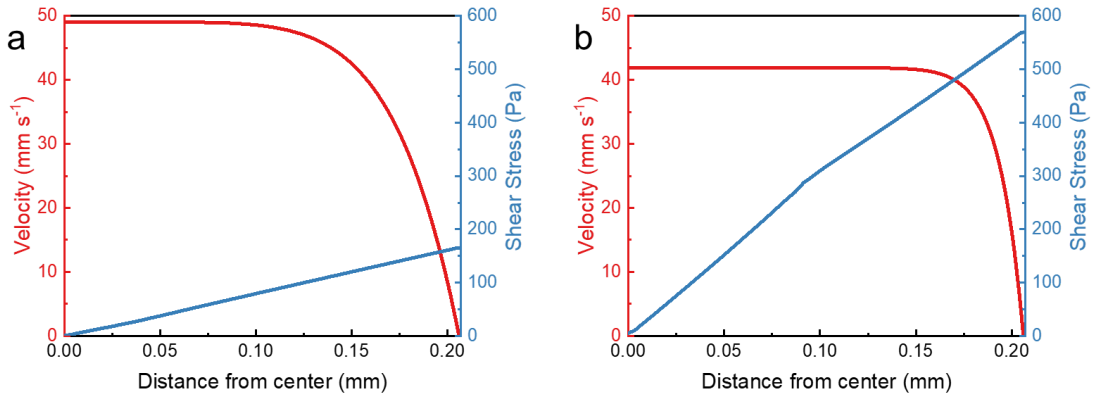

Supplementary Figure 2. Distribution of velocity and shear stress at the nozzle in the printing of (a) pure GO aerogel and (b) GO aerogel with 160 mM ascorbic acid, printed at 300 μL min^{-1} with nozzle of 0.413 mm.

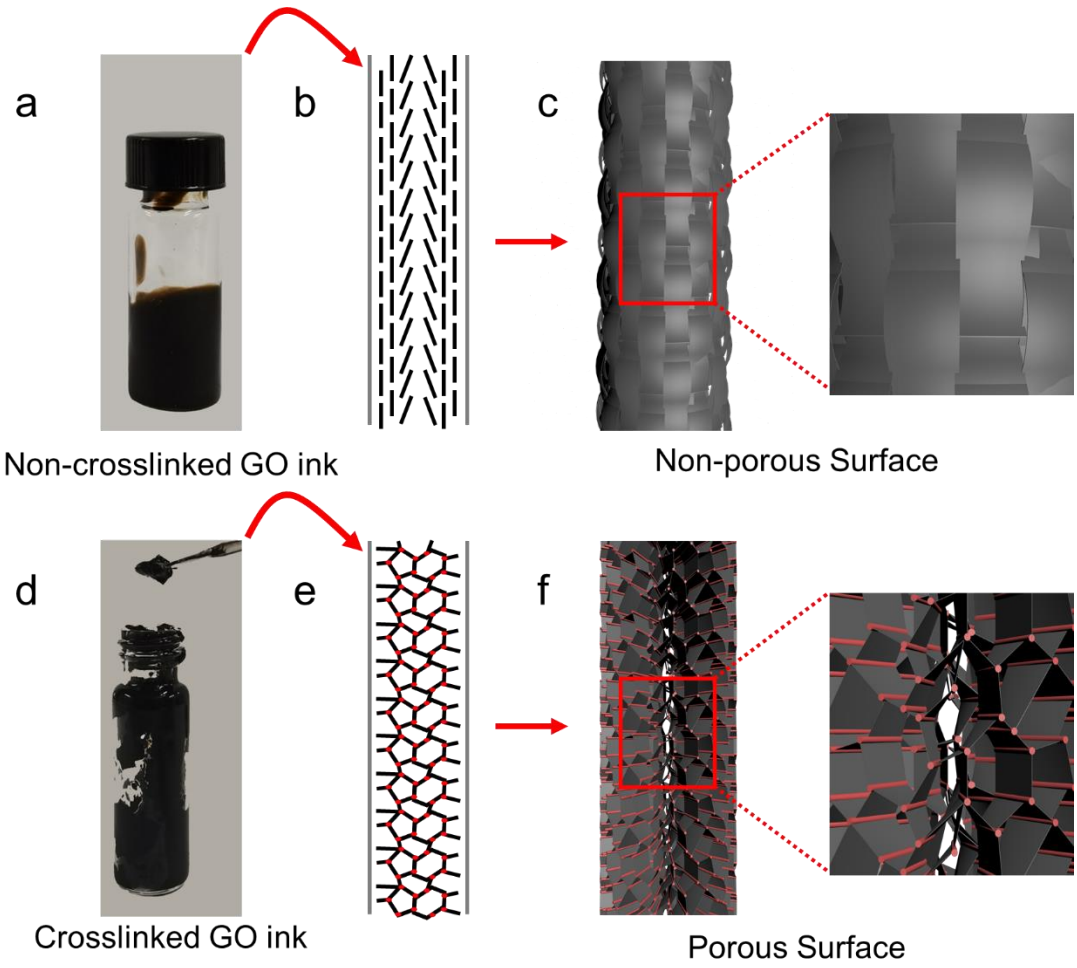

Supplementary Figure 3. The schematic illustration of the influence of crosslinking degree to surface porosity. (a) Photo of pure GO ink. (b) Schematic figure of the printing of non-crosslinked GO ink. (c) Schematic figure of non-porous surface. (d) Photo of GO ink with 160 mM AA. (e) Schematic figure of the printing of crosslinked GO ink. (f) Schematic figure of porous surface printed by crosslinked GO ink. The red lines in (e) and (f) show the crosslinking of the GO flakes.

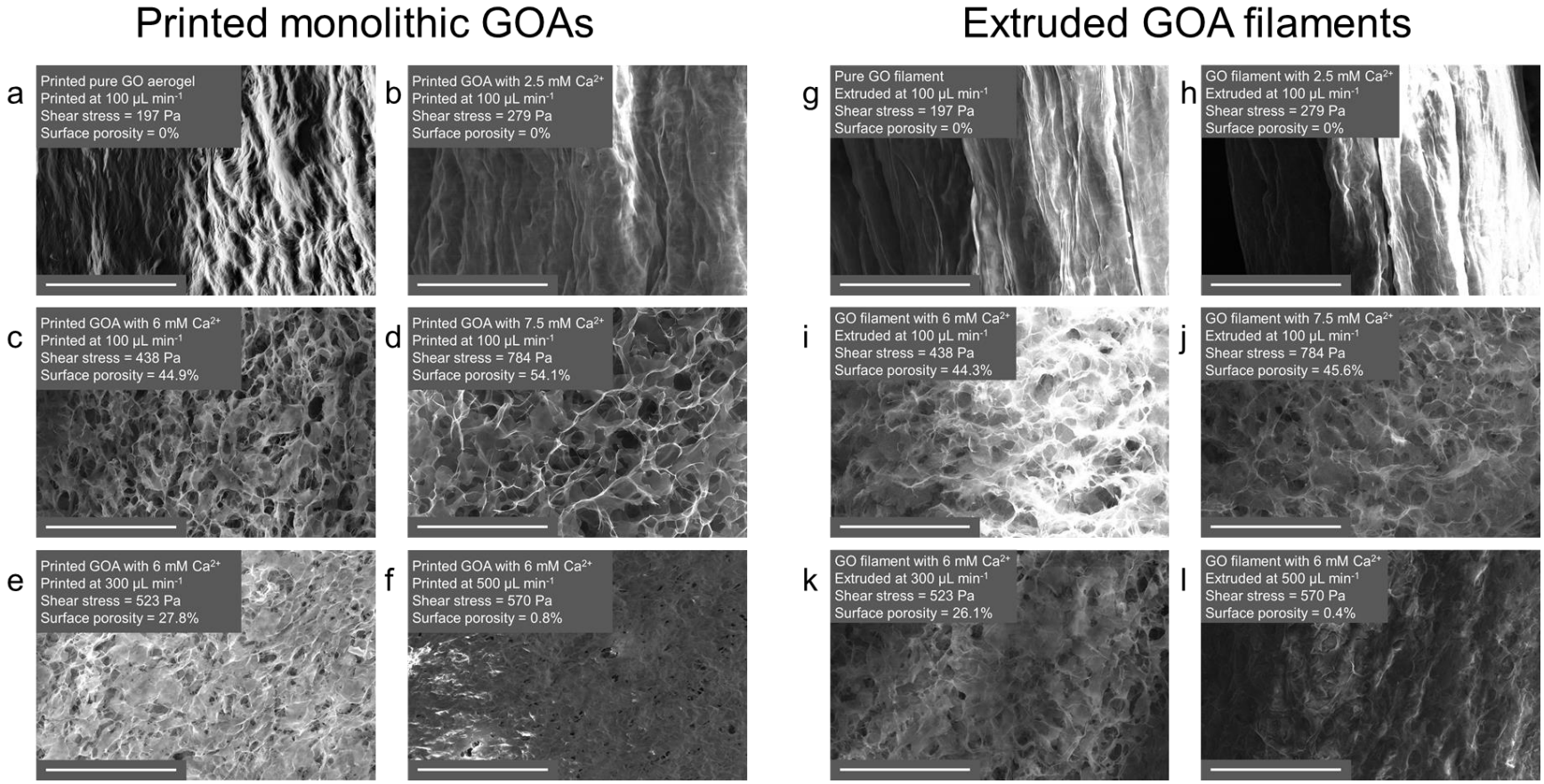

Supplementary Figure 4. SEM figures of (a-f) printed monolithic GO aerogels and (g-l) corresponding extruded GOA filaments with different concentrations of Ca^{2+} and at different flow rates. (a) Surface SEM of printed pure GO aerogel printed at 100 µL min^{-1}. (b-d) Surface SEM of printed monolithic GOAs with (b) 2.5 mM Ca^{2+}, (c) 6 mM Ca^{2+}, and (d) 7.5 mM Ca^{2+}, printed at 100 µL min^{-1}. (e-f) Surface SEM of printed monolithic GOAs with 6 mM Ca^{2+}, printed at (e) 300 µL min^{-1} and (f) 500 µL min^{-1}. (g) Surface SEM of extruded pure GO aerogel filament extruded at 100 µL min^{-1}. (h-j) Surface SEM of GOA filaments with (h) 2.5 mM Ca^{2+}, (i) 6 mM Ca^{2+}, and (j) 7.5 mM Ca^{2+}, extruded at 100 µL min^{-1}. (k-l) Surface SEM of GOA filaments with 6 mM Ca^{2+}, extruded at (k) 300 µL min^{-1} and (l) 500 µL min^{-1}. All the samples are printed/extruded using 0.210 mm nozzle. Surface shear stress are obtained by CFD simulation (see Methods). Scale bars 100 µm.

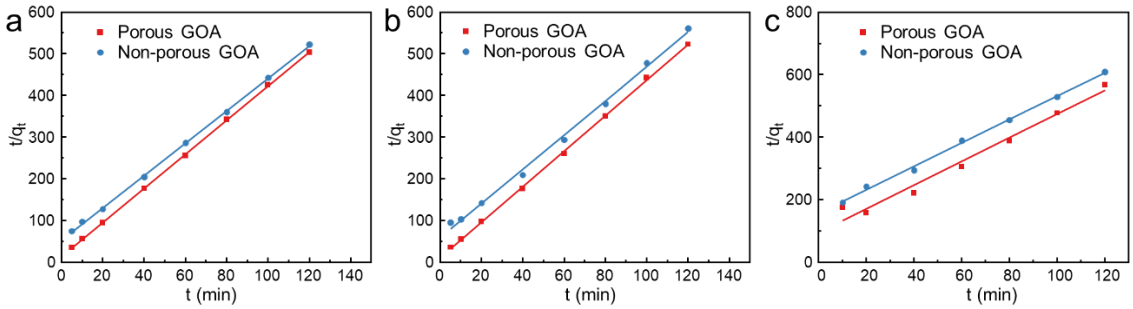

Supplementary Figure 5. Kinetic fitting curves of porous GOA and non-porous GOA in (a) rhodamine B, (b) methylene blue, and (c) malachite green, based on pseudo-second-order model.

Supplementary Table 2. Rate constants and R^2 values of dye adsorption by aerogels.

Dye	Structure	Aerogels	k_2	q_e	R^2
Rhodamine B	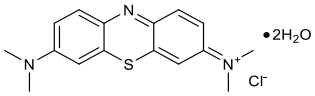	Porous GOA	1.663	0.234	>0.99
		Non-porous GOA	0.282	0.244	>0.99
		Porous GA	0.351	0.0541	0.98
		Non-porous GA	0.0742	0.0713	0.98
Methylene blue	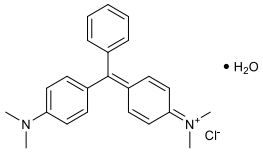	Porous GOA	1.19	0.245	>0.99
		Non-porous GOA	0.286	0.257	>0.99
		Porous GA	0.216	0.796	0.95
		Non-porous GA	0.0592	0.111	0.97
Malachite green	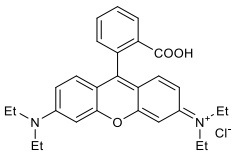	Porous GOA	0.150	0.264	0.97
		Non-porous GOA	0.0897	0.267	>0.99
		Porous GA	0.0386	0.169	0.98
		Non-porous GA	0.0130	0.234	0.96

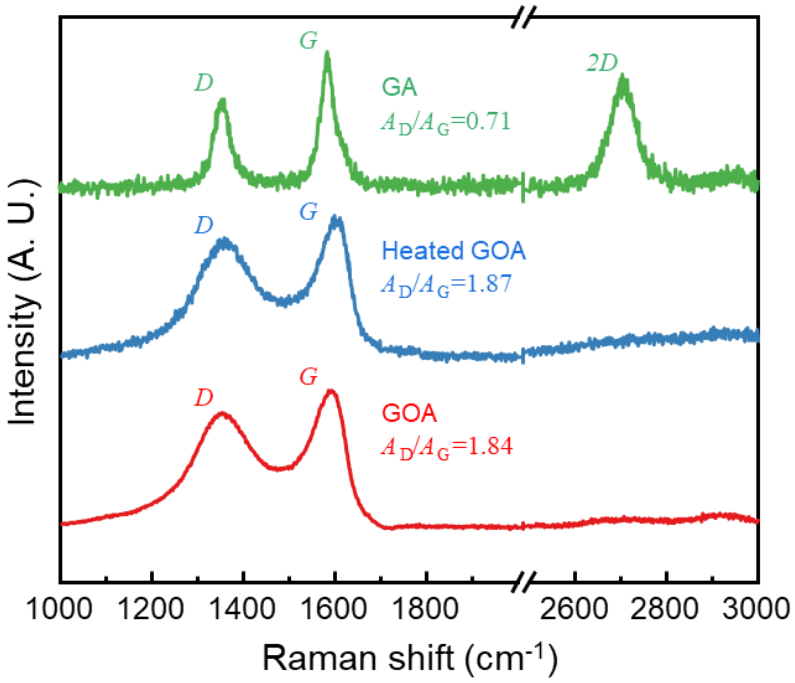

Supplementary Figure 6. Raman spectra of porous GOA, heated porous GOA, and porous GA.

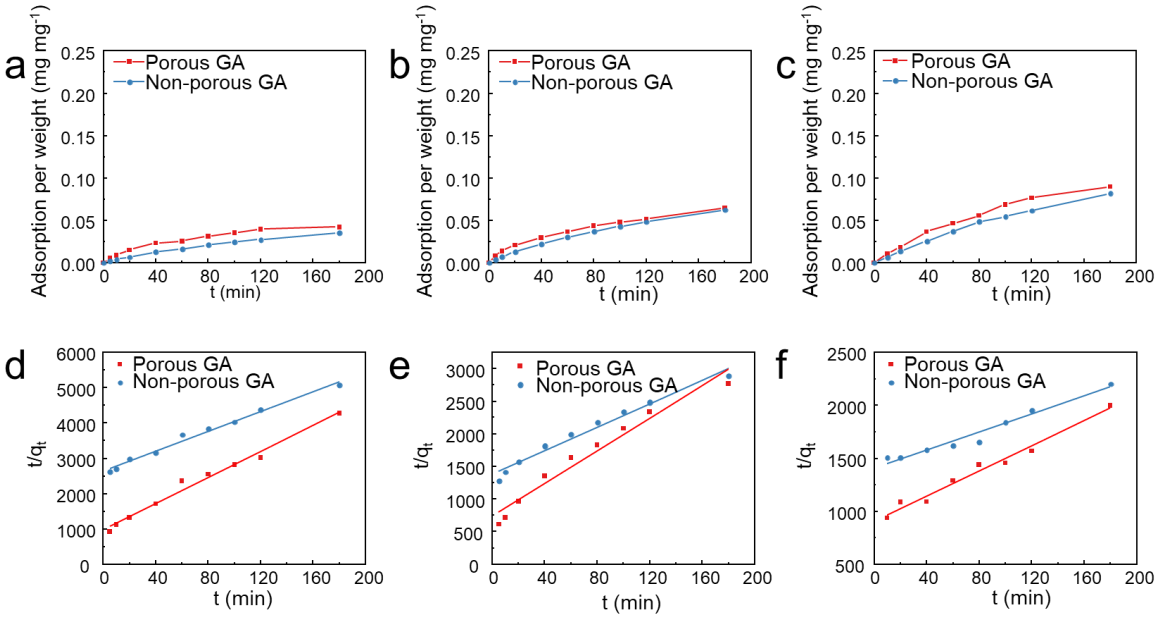

Supplementary Figure 7. (a-c) Dye adsorption curves of porous GA and non-porous GA in (a) rhodamine B, (b) methylene blue, (c) malachite green, and (d-f) corresponding kinetic fitting curves.

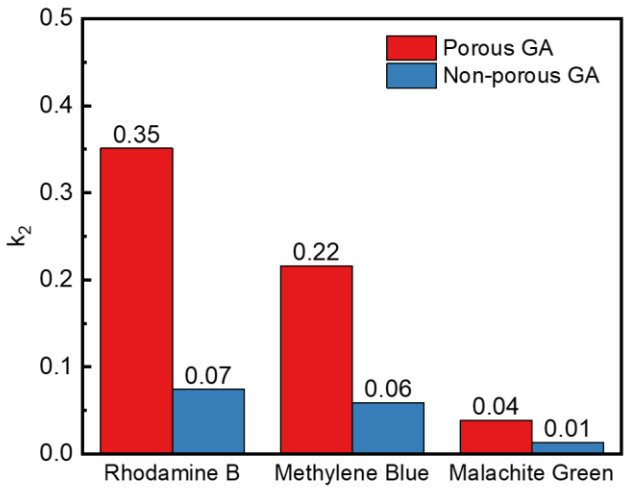

Supplementary Figure 8. Rate constants of dye adsorption by porous GA and non-porous GA.

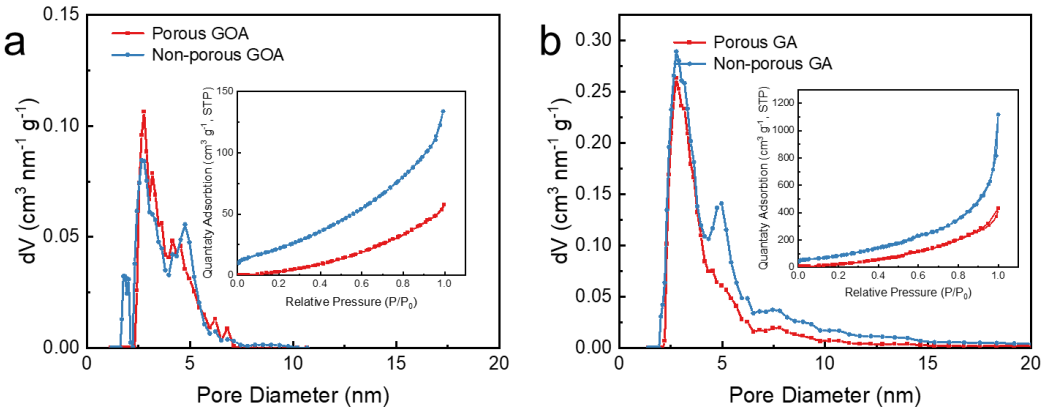

Supplementary Figure 9. Pore size distribution profile and corresponding nitrogen absorption−desorption isotherm (inset) of (a) GOA and (b) GA. The specific surface area is 96.517 m^2 g^{-1} for porous GOA and 107.735 m^2 g^{-1} for non-porous GOA, 288.524 m^2 g^{-1} for porous GA and 326.658 m^2 g^{-1} for non-porous GA.

Supplementary References

1 Peng, M. et al. 3D printing of ultralight biomimetic hierarchical graphene materials with exceptional stiffness and resilience. *Adv. Mater.* **31**, e1902930 (2019).

2 Jiang, Y. et al. Direct 3D printing of ultralight graphene oxide aerogel microlattices. *Adv. Funct. Mater.* **28** (2018).

3 Tang, X. et al. Architectured leaf-inspired $Ni_{0.33}Co_{0.66}S_2$/graphene aerogels via 3D printing for high-performance energy storage. *Adv. Funct. Mater.* **28** (2018).

4 Tang, X. et al. Generalized 3D printing of graphene-based mixed-dimensional hybrid aerogels. *ACS Nano* **12**, 3502-3511 (2018).

5 Zhu, C. et al. Highly compressible 3d periodic graphene aerogel microlattices. *Nat. Commun.* **6**, 6962 (2015).

6 Zhu, C. et al. Supercapacitors based on three-dimensional hierarchical graphene aerogels with periodic macropores. *Nano Lett.* **16**, 3448-3456 (2016).

7 Zhang, Q. et al. 3D printing of graphene aerogels. *Small* **12**, 1702-1708 (2016).

8 Qi, Z. et al. 3D-printed, superelastic polypyrrole-graphene electrodes with ultrahigh areal capacitance for electrochemical energy storage. *Adv. Mater. Technol.* **3** (2018).

9 Ma, J., Wang, P., Dong, L., Ruan, Y. & Lu, H. Highly conductive, mechanically strong graphene monolith assembled by three-dimensional printing of large graphene oxide. *J. Colloid Interface Sci.* **534**, 12-19 (2019).

10 Yao, B. et al. 3D-printed structure boosts the kinetics and intrinsic capacitance of pseudocapacitive graphene aerogels. *Adv. Mater.* **32**, e1906652 (2020).